Check for updates

TUBERCULOSIS

Copyright © 2025 The Authors, some rights reserved; exclusive licensee American Association for the Advancement of Science. No claim to original U.S. Government Works

Rapid tuberculosis diagnosis from respiratory or blood samples by a low cost, portable lab-in-tube assay

Brady M. Youngquist[1,2], Julian Saliba[1,2], Yelim Kim[1,2], Thomas J. Cutro[3], Christopher J. Lyon[1,2], Juan Olivo[4], Ngan Ha[5], Janelle Fine[6], Rebecca Colman[6], Carlos Vergara[4], James Robinson[7], Sylvia LaCourse[8,9,10], Richard S. Garfein[6], Donald G. Catanzaro[11], Christoph Lange[12,13,14,15], Eddy Perez-Then[4], Edward A. Graviss[5], Charles D. Mitchell[16], Timothy Rodwell[6], Bo Ning[1,2], Tony Y. Hu[1,2]*

Rapid portable assays are needed to improve diagnosis, treatment, and reduce transmission of tuberculosis (TB), but current tests are not suitable for patients in resource-limited settings with high TB burden. Here we report a low complexity, lab-in-tube system that is read by an integrated handheld device that detects *Mycobacterium tuberculosis* (*Mtb*) DNA in blood and respiratory samples from a variety of clinical settings. This microprocessor-controlled device uses an LCD user interface to control assay performance, automate assay analysis, and provide results in a simple readout. This point-of-care single-tube assay uses a DNA enrichment membrane and a low-cost cellulose disc containing lyophilized recombinase polymerase amplification and CRISPR-Cas12a reagents to attain single-nucleotide specificity and high sensitivity within 1 hour of sample application, without a conventional DNA isolation procedure. Assay results obtained with serum cell–free DNA isolated from a cohort of children aged 1 to 16 years detected pulmonary and extrapulmonary TB with high sensitivity versus culture and GeneXpert MTB/RIF results (81% versus 55% and 68%) and good specificity (94%), meeting the World Health Organization target product profile criteria for new nonsputum TB diagnostics. Changes in assay results for serum isolated during treatment were also highly predictive of clinical response. Results obtained with noninvasive sputum and saliva specimens from adults with bacteriologically confirmed pulmonary TB were also comparable to those reported for reference methods. This rapid and inexpensive lab-in-tube assay approach thus represents one means to address the need for point-of-care TB diagnostics useable in low-resource settings.

INTRODUCTION

More than 90% of new tuberculosis (TB) cases occur in low- and middle-income countries that have limited health care infrastructure (*1*). Point-of-care (POC) testing suitable for use in resource-limited settings is necessary to improve TB diagnosis and treatment and stop TB transmission (*2*, *3*). An estimated 4.2 million TB cases were undiagnosed or unreported in 2021 (*2*), largely because of limitations and costs of microbiological and molecular-based TB testing in areas with high disease burden given that these tests require expertise, equipment, and infrastructure that are not available in most resource-limited settings (*4*–*7*). Neither approach is suitable for adaptation to POC testing because culture-based tests require weeks to obtain valid final results, and polymerase chain reaction (PCR)–based tests use multistep workflows and expensive and bulky equipment (*8*, *9*). Affordable and portable POC assays are needed to improve TB diagnosis and treatment in resource-limited settings according to the target product profile (TPP) for TB diagnostics set by the World Health Organization (WHO) (*10*, *11*).

New diagnostic approaches are also needed to improve the scope and scale of TB screening efforts (*12*). Sputum specimens, the reference standard, are useful for diagnosis of pulmonary TB (PTB), but not extrapulmonary TB (EPTB) disease (*13*, *14*). Sputum-based tests have limited diagnostic utility in some at-risk populations with paucibacillary disease (such as young children and people living with HIV) who often have difficulty producing sputum or who produce specimens with low bacterial burden, resulting in low diagnostic sensitivity (*15*–*17*). This is a substantial problem because these patient populations are at increased risk for rapid disease progression and increased mortality (*18*–*20*). The sampling requirements for diagnosing EPTB are also highly invasive, and alternate approaches are needed to permit EPTB diagnosis using minimally invasive specimens that can be collected and analyzed in resource-limited settings (*21*, *22*). New diagnostic tests that can analyze nonsputum specimens are thus needed to improve TB diagnosis in these patient populations (*23*).

Laboratory-based assay systems have been used to diagnose TB using saliva and serum specimens, but no true POC test that uses minimal equipment without DNA extraction is now available (*24*–*28*). Here, we report the design and validation of an inexpensive (approximately $2.70 per sample), handheld, battery-powered

[1]Center for Cellular and Molecular Diagnostics, Tulane University School of Medicine, New Orleans, LA 70112, USA. [2]Department of Biochemistry and Molecular Biology, Tulane University School of Medicine, New Orleans, LA 70112, USA. [3]School of Science and Engineering, Tulane University, New Orleans, LA 70112, USA. [4]O&M Medical School (O&Med), Santo Domingo, 10204, Dominican Republic. [5]Houston Methodist Research Institute, Houston, TX 77030, USA. [6]Department of Medicine, University of California San Diego, La Jolla, CA 92093, USA. [7]Section of Pediatric Infectious Disease, Department of Pediatrics, Tulane University, New Orleans, LA 70112, USA. [8]Department of Medicine, Division of Allergy and Infectious Diseases, University of Washington, Seattle, WA 98195, USA. [9]Department of Global Health, University of Washington, Seattle, WA 98195, USA. [10]Department of Epidemiology, University of Washington, Seattle, WA 98195, USA. [11]Department of Biological Sciences, University of Arkansas, Fayetteville, AR 72701, USA. [12]Department of Clinical Infectious Diseases, Research Center Borstel, Leibniz Lung Center, Borstel, 23845, Germany. [13]German Center for Infection Research (DZIF), Partner Site Hamburg-Lübeck-Borstel-Riems, Borstel, 23845, Germany. [14]Respiratory Medicine and International Health, University of Lübeck, Lübeck, 23562, Germany. [15]Baylor College of Medicine and Texas Children's Hospital, Global Tuberculosis Program, Houston, TX 77030, USA. [16]Department of Pediatrics, Division of Infectious Diseases and Immunology, University of Miami Miller School of Medicine, Batchelor Children's Research Institute, Miami, FL 33136, USA.
*Corresponding author. Email: tonyhu@tulane.edu

Downloaded from https://www.science.org at Tulane University on April 09, 2025

lab-in-tube (LIT)–TB assay that detects *Mycobacterium tuberculosis* (*Mtb*) DNA in patient serum, saliva, and sputum samples with a sample-to-answer time of less than 1 hour and that could be deployed as a POC TB test for multiple TB manifestations. This assay integrates sputum or saliva specimen liquification, *Mtb* bacilli lysis, recombinase polymerase amplification (RPA), and CRISPR detection steps into a single consumable tube that is processed and analyzed by the portable assay device. The assay device can also be used to detect *Mtb* DNA in serum to substantially increase sensitivity in children and patients with EPTB. These consumable assay tubes contain lyophilized solubilization material and a separate matrix embedded with lyophilized RPA and CRISPR reagents to allow sequential specimen solubilization and RPA-CRISPR detection, using two protospacer-associated motif (PAM)–free guide RNAs (gRNAs) for optimized target detection. Our results indicate that this approach can detect adult and pediatric TB, including PTB and EPTB cases, with high sensitivity and specificity when using serum, saliva, or sputum as the diagnostic specimen, suggesting that this approach has strong potential as a POC test for TB diagnosis in resource-limited settings underserved by current methods.

RESULTS

Design and optimization of a LIT assay for detecting active TB

An inexpensive LIT and portable device was developed to detect TB DNA in multiple sample types, including blood, saliva, and sputum. In this approach, a respiratory sample is collected in the assay tube, and the tube is then transferred to the incubator port of the portable device for solubilization (lysis buffer) and inactivation (high temperature). The LIT plunger is then depressed to load the lysate onto the DNA capture membrane and initiate the RPA-CRISPR reaction in this device port, and upon its completion, the tube is transferred to the readout port to detect and analyze the resulting fluorescent assay signal (Fig. 1A). The consumable LIT insert for this device holds lyophilized sample liquification chemicals (lysis buffer), a DNA binding membrane necessary for sample processing, and the lyophilized RPA and CRISPR-Cas12a reagents needed for *Mtb* DNA detection (Fig. 1B). The portable rechargeable battery-powered assay device is controlled by a touch screen user interface and contains a laser, fluorescent imaging filters, a camera to read the assay, and a Raspberry Pi microprocessor to integrate fluorescent imaging and automated analysis (Fig. 1, C and D). This assay requires 1 hour to perform the thermal sample lysis, RPA-CRISPR incubation, and fluorescent imaging steps required to return assay results.

Development and optimization of the single-reaction *Mtb* DNA detection assay

POC tests minimize user interventions to eliminate the need for skilled operators and reduce user error and assay variation according to WHO TPP for nonsputum diagnostic tests (table S1) (*11*, *29*). POC tests often use matrices that fluoresce at the excitation wavelength of fluorescein amidite (FAM)–labeled oligonucleotide probes used in CRISPR assays, which can mask assay signal; however, the signal-to-noise ratio can be greatly improved by using cyanine5 (Cy5)–labeled probes (fig. S1).

Single-tube RPA and CRISPR assay conditions were optimized by adjusting the RPA-to-CRISPR activity ratio to avoid premature target cleavage, which can reduce amplicon accumulation required for RPA efficiency and CRISPR cleavage kinetics required for sensitive target detection. Because nonconsensus PAM sequences reduced CRISPR cleavage activity, we examined assay signal produced

Downloaded from https://www.science.org at Tulane University on April 09, 2025

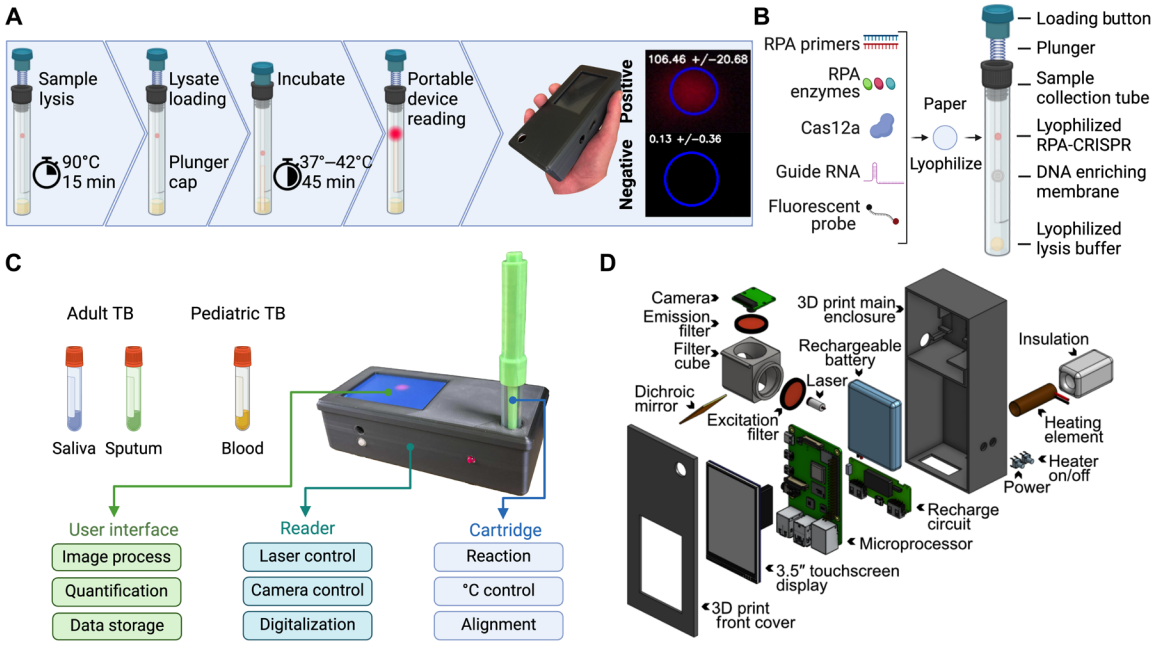


Fig. 1. Schematic of a CRISPR-based POC TB diagnostic device that detects *Mtb* DNA in multiple specimen types. (**A**) LIT-TB assay workflow indicating the time required for its sample lysis, lysate loading, assay incubation, and analysis steps. (**B**) Design and components of the LIT-TB assay tube. (**C**) Overview of sample inputs and assay functions of the handheld device to process the diagnostic specimen and capture and analyze the assay results. (**D**) A 3D rendering of the components of the POC LIT assay device.

in reactions using gRNAs targeting amplicon sequences with (gRNA1) and without (gRNA2 and gRNA3) consensus PAM sites (Fig. 2A, table S2, and fig. S2). Reactions that used gRNAs that did not target consensus PAMs (gRNA2 and gRNA3) yielded higher signal compared with gRNA1 alone, although gRNA1 (consensus PAM) and gRNA2 differed only by a 1–base pair shift. CRISPR signal can also be enhanced by using multiple gRNAs that recognize non-overlapping sites on a target amplicon. The signal did not differ between reactions performed with equal total amounts of gRNA1 + gRNA2 or gRNA1, likely because of recognition site competition and gRNA1-mediated amplicon depletion. Reactions performed with gRNA1 + gRNA3 also did not exhibit greater signal than those that used gRNA3 alone, and such increases were detected only in reactions using gRNA2 + gRNA3. Subsequent assays were thus performed with gRNA2 + gRNA3. CRISPR reaction efficiency was also adjusted by selecting the best reaction temperature and the best Cas12a enzyme, reaction buffer, and gRNA concentration for the assay (Fig. 2B and fig. S3, A to C). These analyses found that the maximum signal was detected at 37°C in reactions performed without added CRISPR buffer and containing a 42 nM concentration of a Cas12a/gRNA2 + 3 complexes, and these conditions were used for all further analyses.

Several matrices were next evaluated for their ability to preserve the activity of the lyophilized assay reagents, because POC TPP tests should permit transportation and storage under ambient conditions. RPA-CRISPR reagents were absorbed on these matrices, flash-frozen in liquid nitrogen, lyophilized to dryness, stored under vacuum with desiccant, rehydrated with an *Mtb* DNA standard solution, and then analyzed for CRISPR signal production using standard assay conditions (Fig. 2C). CRISPR signal detected from a reagent-loaded cotton-based blot paper matrix was >2.5-fold stronger, and the signal tended to rise and plateau earlier than signals detected with other matrices, with >50% maximum signal detected by 30 min after reconstitution. Cellulose-based Whatman paper matrices produced weak signal and variable kinetics that did not align with their pore size or thickness differences, whereas the nitrocellulose or polyethersulfone matrices did not reveal any appreciable CRISPR activity after reconstitution. Cotton-based blot paper was therefore selected as the best reagent matrix for our RPA-CRISPR assay.

To enhance lyophilization stability, we tested the addition of a range of excipients to the reaction mixture and incubated the mixtures at 40°C for 72 hours to mimic high temperatures during transportation. Reagents lyophilized with sugar excipients retained the most activity after 40°C storage in this analysis (fig. S4). We therefore compared the signal detected after reagents were stored for 72 hours at 40°C and −20°C after lyophilization with sucrose, trehalose, sucrose and dextran, or trehalose and dextran (fig. S5). Signals produced by reagents lyophilized with sucrose or trehalose and dextran did not differ within or between these groups after storage at 40°C or −20°C ($P > 0.05$). Reagents lyophilized in trehalose retained less activity than those lyophilized in sucrose ($P < 0.05$), but activity losses did not differ between the two storage temperatures ($P > 0.05$). However, reagents lyophilized with sucrose and dextran or without an excipient revealed large temperature-dependent losses (fig. S5). To characterize the long-term storage characteristics of this assay, RPA-CRISPR reagents were lyophilized in sucrose and stored for up to 3 months at room temperature (RT), 4°C, and −20°C. After 1 month, samples stored at 4°C or RT produced fluorescent signal that fell within the 95% confidence interval (CI) of reagents stored at −20°C (Fig. 2D). After a 2-month storage period, two of the three 4°C and RT-stored reagent sample replicates also fell within the 95% CI of the −20°C reagents. However, after 3 months, the RT-stored reagents produced substantially less signal, and two of the three 4°C reagent samples fell below the 95% CI.

Design of an integrated incubator and imaging device for the POC LIT-TB assay

Our LIT-TB assay workflow required a device that could maintain an optimal temperature to maximize signal and minimize variability and capture and quantify the assay signal. We therefore fabricated a 3D-printed handheld device to contain a miniature incubator and several imaging components [light-emitting diode (LED), optical filters, dichroic mirror, and image sensor] controlled by a Raspberry Pi microprocessor and a 3.5-inch (8.89 cm) touchscreen (Fig. 2E and tables S3 and S4). Most device functions were achieved with available parts, but the miniature incubator was generated by using the microprocessor to control a resistance heater that contacted an assay tube surrounded by insulation. Heating efficiency analyses performed without insulation or with styrofoam, polyethylene foam, or pine wood led to the selection of styrofoam insulation because of its superior performance in permitting a rapid temperature increase in the assay tubes (Fig. 2F and fig. S6). Next, the temperature gradient was mapped in an assay tube containing 1 ml of a 65°C aqueous specimen to detect the 37°-to-42°C region required for optimal RPA-CRISPR activity, which identified a position 3.25 cm from the tube base that consistently matched this temperature (range: 38.0° to 41.6°C; mean ± SD: 40.19° ± 1.14°C) over 20 replicates, and assay fluorescent images were captured at this height to simplify the assay workflow (fig. S7).

The image capture assembly of this device was created from readily available parts, and an algorithm was generated to determine the region of interest (ROI) for signal quantification by refining the parameters governing the signal detected within a fixed circular region corresponding to the position of the assay reagents (Fig. 2G). This was done by comparing the signal intensity of a radius (I_x) to the signal intensity from radii of increasing size (I_{x+n}) to find the optimal radius size for quantification. This was centered at the geometric midpoint of the laser focus using the fixed position of the optical components to ensure a consistent position. An intensity threshold was then applied to shrink this radius to minimize the number of pixels that did not differ from background signal detected outside this region, with signal detected outside this radius treated as noise to mitigate potential interference, which was largely eliminated by use of assay tubes with opaque caps (fig. S8). This approach reliably detected signal ROIs allowing robust data collection and analysis for accurate diagnosis and displayed annotated assay images for the assay operator.

LIT-TB dynamic range, cross-reactivity, and detection of common drug resistance mutation

The LIT-TB signal detected with DNA isolated from healthy serum spiked with serial dilutions of *Mtb* genomic DNA exhibited a broad linear range (0.05 to 5000 pg/μl), even for signal not visible by eye on the captured image (Fig. 2, H and I). We found that no substantial signal was detected in samples spiked with genomic DNA from other mycobacteria species that cause human respiratory disease, consistent with the *Mtb*-specific design of the assay primers and

Downloaded from https://www.science.org at Tulane University on April 09, 2025

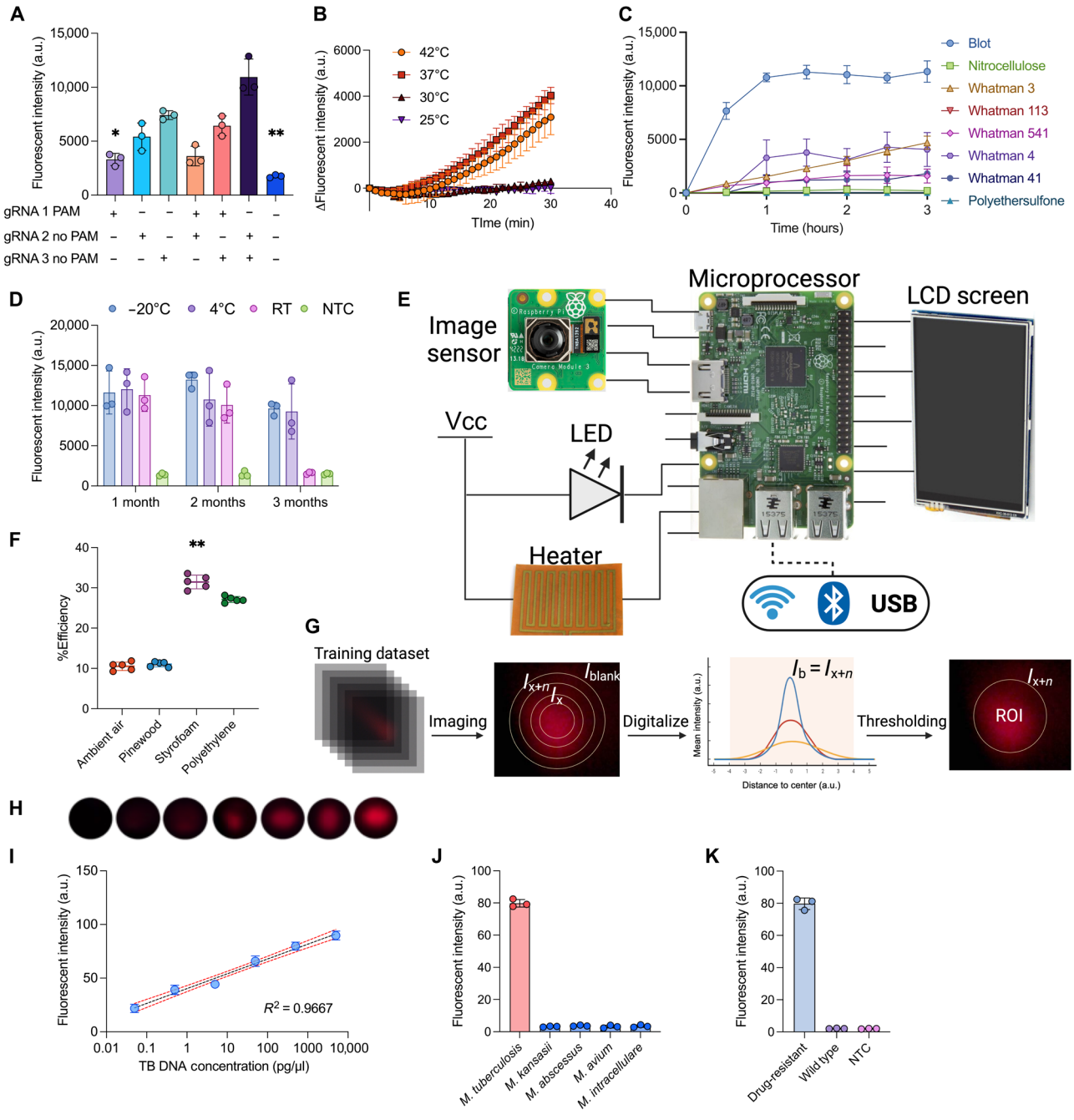


Fig. 2. RPA-CRISPR assay optimization and portable device development. (**A**) Signal produced by RPA-CRISPR reactions using gRNAs with (gRNA1) or without consensus PAM sequences (gRNA2 and gRNA3). $n = 3$. $^{*}P < 0.05$ and $^{**}P < 0.01$ versus gRNA2 + gRNA3 by Kruskall-Wallis test with Dunn's test for multiple comparisons. (**B**) Evaluation of gRNA2 + gRNA3 multiplex assay performance at different temperatures. $n = 3$. (**C**) RPA-CRISPR reaction kinetics for *Mtb* DNA detection when using RPA-CRISPR reagents lyophilized on different support matrices over time. $n = 3$. (**D**) Storage temperature effects on lyophilized RPA-CRISPR reagent activity. NTC, no template control. $n = 3$. (**E**) Circuit diagram of the microprocessor connections controlling image sensor, LED, heater, LCD screen, and wireless output components of the assay device. Vcc, voltage at the common collector. (**F**) Heating efficiency values with different insulating materials in the LIT incubator port. $n = 5$. $^{**}P < 0.01$ versus ambient air by Kruskall-Wallis test with Dunn's test for multiple comparisons. (**G**) Workflow used to optimize ROI detection. Training data images were assessed by shrinking a circle centered on the fixed position of the LIT-TB reagents to exclude mean pixel values that do not differ from background noise. Radii of varying size were compared to identify the optimal size of the ROI for analysis. I_x, intensity for a given radius x; I_{x+n}, intensity for a radius x plus n; I_{blank}, intensity of the background (no-template control); I_b, mean intensity for a given distance n radius away from the center. (**H**) Representative images of the detection ROI with RPA-CRISPR signal and (**I**) a concentration curve generated with DNA isolated from healthy serum spiked with serial dilutions of *Mtb* DNA. The black dotted line is the linear regression best-fit line, and red dotted lines are the 95% CI. $n = 3$. (**J**) Signal detected in RPA-CRISPR assays performed with DNA isolated from *Mtb* and other mycobacteria species. $n = 3$. (**K**) RPA-CRISPR assay specific for a drug-resistant mutant (*rpoB* S450L) performed using DNA from drug-resistant mutant *Mtb*, wild-type *Mtb*, or NTC. $n = 3$. Data in (A) to (D), (F), (J), and (K) are presented as means ± SD, and dots in (A), (D), (F), (J), and (K) represent replicates. a.u., arbitrary units.

Downloaded from https://www.science.org at Tulane University on April 09, 2025

gRNAs (Fig. 2J). An alternate assay variant reproducibly detected a common single-nucleotide polymorphism (*rpoB* S450L) associated with *Mtb* resistance to rifampin, an important first-line anti-TB drug (Fig. 2K) (*30*, *31*). Single-nucleotide specificity was achieved by two approaches, first, by aligning the gRNA "seed" region with this mutation, because this region is essential for optimal Cas12a binding and trans-cleavage activity. Second, this gRNA sequence was modified to introduce a single nucleotide mismatch in a conserved sequence region so that Cas12a binding to the wild-type allele required an additional gRNA mismatch.

LIT-TB results detected with serum DNA sensitively diagnose pediatric PTB and EPTB

Sputum is the primary diagnostic specimen for PTB diagnosis, but young children, individuals living with HIV or other immune insufficiencies, and individuals with EPTB often cannot produce sputum or produce sputum with low *Mtb* concentrations that yield false negatives results (*32*–*34*). *Mtb* DNA can be detected in the sera of patients with TB by a sensitive laboratory-based CRISPR assay (*24*), and we therefore analyzed LIT-TB performance using cell-free DNA isolated from sera of a pediatric TB cohort enrolled in the Dominican Republic. This cohort contained 27 children diagnosed with PTB or EPTB (one patient was diagnosed with both PTB and EPTB) who were classified as having "confirmed" and "unconfirmed" TB on the basis of microbiologic or clinical evidence, respectively; and 35 children who were close contacts but did not demonstrate evidence of *Mtb* infection and were tuberculin skin test (TST) negative (tables S5 and S6 and fig. S9). Confirmed TB was classified as children with bacteriological confirmation of TB (culture or GeneXpert positive). Unconfirmed TB was classified as children with no bacteriological confirmation but meeting at least two of the following criteria: symptoms suggestive of TB, a chest x-ray consistent with TB, TB exposure or immunological evidence of *Mtb* infection, or a positive response to TB treatment. Serum *Mtb* DNA signals detected for treatment-naïve patients with TB had similar high sensitivity for TB (81%; 22 of 27 cases), PTB (83%; 15 of 18), and EPTB (75%; six of eight), all of which exceeded those obtained by sputum, induced sputum, or gastric lavage cultures (55%; five of nine) or by GeneXpert MTB/RIF (Xpert) (68%; 15 of 22). Sensitivity also did not significantly differ between confirmed (92%; 11 of 12 cases; 95% CI: 61.5 to 99.8) and unconfirmed PTB cases (75%; four of six cases; 95% CI: 22.3 to 95.7) (Fig. 3A). In the Dominican Republic cohort, serum LIT-TB, sputum Xpert, and culture results detected 23, 15, and 5 cases, respectively; eight were serum LIT-TB positive only, one was sputum Xpert positive only, and four were diagnosed by other clinical findings (fig. S10). Serum LIT-TB results were positive for 78% (seven of nine) of EPTB or PTB plus EPTB cases, which otherwise required tissue biopsy (tuberculous lymphadenitis), x-ray imagery (Pott's disease and spinal TB), or other clinical observations to diagnose.

Mtb DNA signal was sporadically detected in the first samples of the close contact group (94% specificity; 2 of 35 children) but not in any of their follow-up samples, indicating that repeat testing accurately classified all close contacts as TB negative (Fig. 3B). In sera obtained from children in the United States (New Orleans, Louisiana) who had low likelihood of TB disease but who were not tested for TB, all 49 participants tested negative by LIT-TB (fig. S11). LIT-TB signal tended to decrease after treatment initiation, resulting in a progressive decrease in serum-positive samples from baseline (81% positive) to the first, second, and third intervals after treatment initiation (46, 25, and 6% positive) (Fig. 3C and figs. S12 and S13). Similar results were observed in the confirmed PTB and unconfirmed PTB groups, and patients with EPTB had a significant drop ($P < 0.05$) in signals from samples taken 6 to 12 weeks after treatment compared with baseline (Fig. 3D).

Results from several cases highlight the advantages of serum LIT-TB assay results for TB diagnosis or treatment monitoring. For example, a 4-year-old male diagnosed with lymphatic EPTB by a biopsy that revealed granulomatous lymphadenitis with caseating necrosis who was LIT-TB positive at TB diagnosis converted to and remained negative after treatment initiation, consistent with a positive-to-negative chest x-ray conversion (Fig. 3E). In addition, a 3-year-old male diagnosed with both PTB and lymphatic EPTB had continued EPTB throughout treatment (up to 8 weeks posttreatment), and LIT-TB signal gradually declined throughout treatment until becoming negative at 35 weeks when a clinical response was observed (Fig. 3F). By contrast, a 12-year-old male diagnosed with rifampin-resistant PTB by Xpert and treated with moxifloxacin, clofazimine, ethionamide, cycloserine, and bedaquiline did not exhibit clinical response or serum LIT-TB conversion by 10 weeks after treatment initiation but had negative values for both at the fourth study visit 27 weeks after treatment initiation (Fig. 3G). Persistent serum LIT-TB, symptoms, and chest x-ray results consistent with TB were also detected in a 15-year-old female with confirmed PTB who stopped treatment after 4 weeks, and these values did not convert until after she reinitiated treatment at 10 weeks postdiagnosis because of progression of her TB symptoms (Fig. 3H).

Development of the RPA-CRISPR–compatible respiratory sample processing procedure

Noninvasive respiratory specimens, such as sputum and saliva, could be more enriched for *Mtb* bacilli and *Mtb* DNA than blood and were therefore analyzed using LIT-TB assay tubes modified to contain chemicals that can reduce the viscosity of these specimens and lyse *Mtb* bacilli (Fig. 4A). NaOH, dithiothreitol (DTT), and isopropanol all liquefied these samples, either alone or in combination, as measured by a reduction in absorbance (Fig. 4B). DTT, which dissociates disulfide bonds, lacked the denaturing effects of the other materials, had similar effects on saliva (figs. S14 and S15), and was thus selected for further use. Next, the temperature necessary for complete heat-induced *Mtb* killing was determined by heat-treating *Mtb* H37Rv strain bacilli [4.6×10^7 colony-forming units (CFU)/ml] spiked into artificial sputum. Complete sterilization was observed after samples were incubated at 80°C for 15 or 30 min as illustrated by lack of colony growth on agar plates (fig. S16). A 15-min 90°C incubation was selected for sample inactivation because of the variable heat killing performance reported at 80°C in the literature (*35*–*37*).

The complete LIT-TB design should directly capture *Mtb* DNA from liquified sputum or saliva lysates and rehydrate lyophilized assay reagents to initiate an RPA-CRISPR reaction. Nucleic acid capture onto cellulose-backed porous membranes has been described previously and has potential to permit one-step capture of DNA from patient samples that is compatible with nucleic acid amplification–based tests (*38*–*40*). *Mtb* DNA-spiked sputum lysates were added to DNA capture/transfer membranes, rinsed, and transferred to RPA-CRISPR detection membranes. Polyethersulfone (PES) and cellulose-based Whatman membranes supported similar

Downloaded from https://www.science.org at Tulane University on April 09, 2025

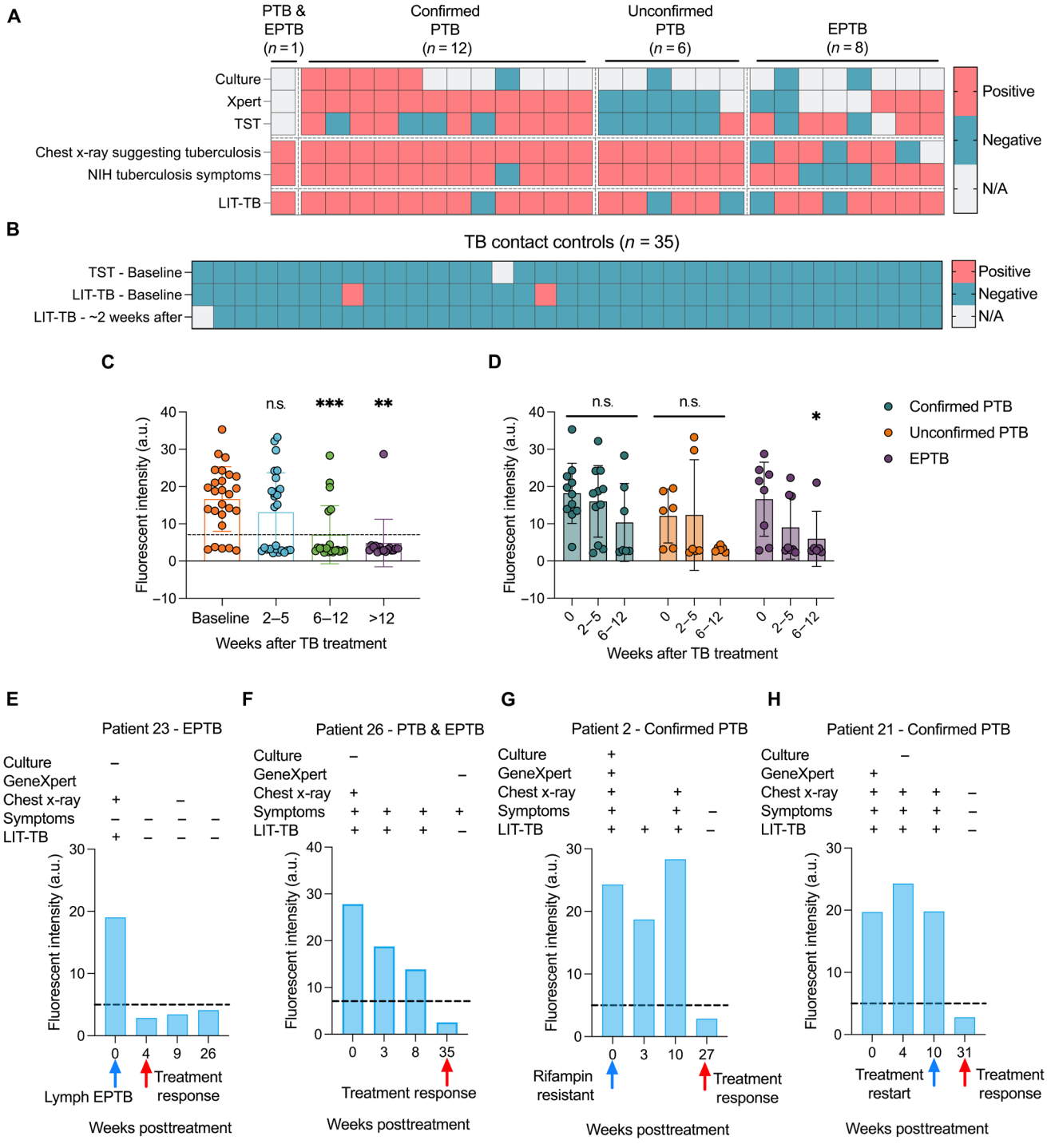


Fig. 3. LIT-TB assay performance with pediatric TB cohort serum samples. (**A**) Clinical findings and LIT-TB results for different TB subgroups. N/A, not available. $n = 1$, PTB and EPTB; $n = 12$, confirmed PTB; $n = 6$, unconfirmed PTB; $n = 8$, EPTB. (**B**) TST and serial LIT-TB results in pediatric close contacts of the TB cohort. $n = 35$. (**C**) Serum LIT-TB signals at baseline and after treatment for all TB cases with follow-up samples ($n = 26$). (**D**) Serum LIT-TB signals over time in confirmed PTB ($n = 11$), unconfirmed PTB ($n = 6$), and EPTB ($n = 8$) cases before and after treatment initiation. Data in (C) and (D) are presented as means ± SD, where the dashed line denotes the positive signal threshold. $^*P < 0.05$, $^{**}P < 0.01$, and $^{***}P < 0.001$ versus baseline by Welch ANOVA with Dunnett's T3 test for multiple comparisons. n.s., not significant. (**E** to **H**) Clinical findings and serum LIT-TB results before and after anti-TB treatment initiation for a child with EPTB who had rapid treatment responses (E), a child with PTB and EPTB who displayed EPTB symptoms through 8-week posttreatment initiation with clinical response at week 35 (F), and children with confirmed TB who had drug resistance (G) or were noncompliant with the treatment regimen between 4 and 10 weeks posttreatment initiation but exhibited treatment response after adjusted treatment or increased compliance (H). Positive signal threshold (dashed line) was calculated using mean plus SD of triplicate NTC samples. Data represent single LIT-TB results in the designated patients at the indicated time points. NIH, National Institutes of Health.

Downloaded from https://www.science.org at Tulane University on April 09, 2025

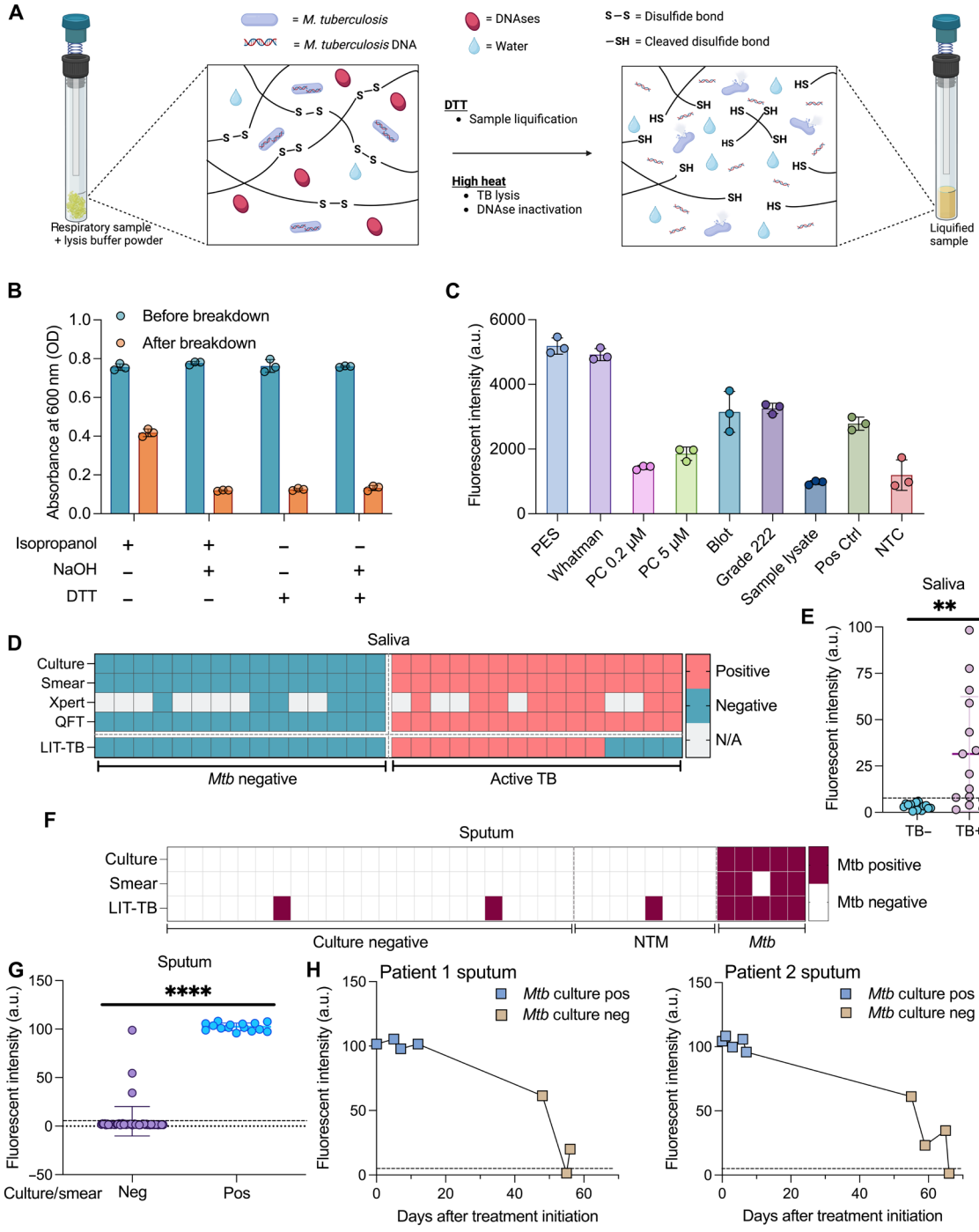


Fig. 4. LIT-TB diagnostic performance with direct saliva and sputum specimens obtained from adult TB cohorts. (**A**) Schematic of in-tube sputum and saliva liquification by DTT and heat-mediated DNAse and *Mtb* inactivation and *Mtb* lysis. (**B**) Sputum absorbance at 600 nm before and after a 10-min RT incubation with the indicated chemicals, where decreased absorbance indicates sputum solubilization. $n = 3$ replicates per condition. (**C**) RPA-CRISPR fluorescent signal detected after assay DNA capture discs made from different materials were incubated with *Mtb* DNA-spiked sputum lysates, rinsed, and added to RPA-CRISPR reactions. PC, polycarbonate. $n = 3$ replicates per condition. (**D**) Clinical findings and saliva LIT-TB results for a case-control TB cohort and (**E**) relative fluorescent intensity detected for these samples. $^{**}P < 0.01$ by Welch's *t* test. $n = 15$, *Mtb* negative; $n = 15$, active TB. (**F**) Clinical findings and sputum LIT-TB results for a cohort of individuals diagnosed with TB disease or NTM infections or with no evidence of *Mtb* infection and (**G**) relative fluorescent intensity detected for these samples. $^{****}P < 0.0001$ by Welch's *t* test. $n = 23$, culture negative; $n = 8$, NTM; $n = 5$, *Mtb*. (**H**) Sputum LIT-TB signal detected for two patients with TB with serial samples collected at ≤2 and ≥ 6 weeks after anti-TB treatment initiation. Positive signal thresholds for saliva and sputum cohorts were calculated by the mean plus three times the SD of triplicate NTC normal saliva and artificial sputum samples. Optimization experiments were run in triplicate, and patient testing results were obtained from a single LIT-TB test. Data in (B), (C), (E), and (G) are presented as means ± SD; dots represent individual samples. Schematic illustration created with BioRender. OD, optical density.

Downloaded from https://www.science.org at Tulane University on April 09, 2025

performance in this analysis (Fig. 4C). We next evaluated whether RPA-CRISPR signal derived from membranes that were or were not subjected to this wash step and found that it was required for maximum signal production only when using the Whatman membrane, suggesting this matrix transferred RPA-CRISPR reaction inhibitors without this rinse (fig. S17). We therefore used a sandwich approach where Whatman paper was used as a support matrix to attach the PES membrane to the assay pluger. In this design, double-sided tape was used to affix the Whatman matrix to both materials and had a punched-out region between the PES and Whatman layers to allow the sample to wick into the Whatman matrix to enhance DNA absorption on the PES membrane surface facing this sample.

A 3D-printed plunger was designed to hold the DNA enrichment membrane and RPA-CRISPR reagent membranes to permit DNA capture and target detection within sealed LIT-TB tubes and protect the user from *Mtb* exposure (fig. S18). After collecting the sample in this tube, pressing this plunger (first click) lowers the DNA capture membrane into the heat-inactivated sample lysate. Pressing this plunger again (second click) raises this DNA capture membrane above the lysate and brings it into contact with an RPA-CRISPR reagent–loaded membrane carried by the inner shaft of the plunger. This action allows the transfer of captured cell-free DNA that initiates the RPA-CRISPR reaction (data file S1 and movie S1).

LIT-TB analysis of an standard curve generated by spiking artificial sputum with serial dilutions of *Mtb* H37Rv yielded a limit of detection (LoD; 78.1 CFU/ml) for this assay (fig. S19) comparable to LoDs reported for GeneXpert MTB/RIF (130 CFU/ml) and GeneXpert Ultra (15.6 CFU/ml) (*41*). Comparison of this LoD (78.1 CFU/ml) to a standard curve generated with a plasmid containing the IS6110 target of the LIT-TB assay found that this LoD corresponded to 38.2 IS6110 copies/μl and thus 2.4 *Mtb* genomes/μl, given that the *Mtb* H37Rv genome contains 16 copies of the IS6110 insertion element.

LIT-TB POC assay performance with saliva and sputum samples from two adult TB cohorts

Saliva from a case-control cohort of 15 adults diagnosed with TB disease and 15 who lacked evidence of *Mtb* infection was analyzed by LIT-TB POC assay operators blinded to sample reference results. This analysis detected 11 true-positive signals [73% sensitivity (95% CI: 44.9 to 92.2)], with no false positives [100% specificity (95% CI: 78.2 to 100)] (Fig. 4D), although fluorescent signals from the TB-positive samples varied widely (Fig. 4E). Similar LIT-TB POC assay results were obtained upon analysis of 71 sputum samples obtained from 36 adults (≥18 years) with suspected TB. Diagnostic sensitivity by LIT-TB was high [100% (95% CI: 47.8 to 100), five of five cases], and specificity [90.3% (95% CI: 74.3 to 98.0), 28 of 31 controls] was similar for individuals with nontuberculous mycobacteria (NTM) infections [87.5% (95% CI: 47.4 to 99.7), seven of eight cases] or no evidence of *Mtb* infection [91.3% (95% CI: 72.0 to 98.9), 19 of 21 individuals] (Fig. 4F and table S7). All (15 of 15) *Mtb* culture–positive samples were LIT-TB positive, whereas 3 of 56 *Mtb* culture–negative samples had LIT-TB false-positive results (Fig. 4G). True-positive and true-negative fluorescent intensity signals were highly divergent [105.2 ± 2.5 versus 1.9 ± 0.5 relative fluorescence units (RFU)], whereas false positives revealed intermediate values (range, 34.3 to 99.0 RFU). Sputum LIT-TB signals were also highly consistent among sequential pretreatment samples available for a subset of individuals, except in one individual diagnosed with an NTM infection who had two true negatives and one false positive suggestive of sample contamination (fig. S20). However, serial pretreatment samples were not available for the other two individuals with false-positive results. Last, two patients who had available sputum collected at ≤2 weeks and ≥ 6 weeks posttreatment initiation revealed consistent signals within the early treatment that which decreased during later treatment (Fig. 4, H and I, and figs. S21 and S22).

DISCUSSION

Our results indicate that a user-friendly POC TB diagnostic assay system can analyze serum and respiratory samples for robust diagnosis of PTB and EPTB in nonclinical settings. *Mtb* DNA concentrations can be very low in serum versus respiratory specimens, but serum *Mtb* DNA can diagnose both PTB (*24*) and EPTB (*42*), and thus, serum-based *Mtb* DNA assays are of substantial interest despite their additional sample processing requirements (blood collection, serum/plasma isolation, and DNA extraction). Multiple studies have detected *Mtb* DNA in blood using laboratory assays that are not suitable for POC tests because of their equipment, workflow, and reagent storage requirements (*24*, *25*, *43*), but our proposed LIT approach minimizes many of these issues to make this approach feasible with minimal additional battery-powered equipment. Serum LIT results diagnosed pediatric PTB and EPTB cases with similarly strong performance and decreased in association with symptom improvement after treatment initiation and remained stable or increased during treatment noncompliance or ineffective treatment, suggesting their potential utility for treatment monitoring. Similar on-treatment saliva and sputum samples were not available for this cohort or the other analyzed cohorts but would be expected to have less utility for monitoring treatment clearance because of the known persistence of DNA from nonviable *Mtb* bacilli in respiratory specimens after initiation of effective treatment (*44*, *45*). Nonetheless, LIT sputum results did detect *Mtb* DNA decreases in two individuals with serial samples available at an early and subsequent treatment intervals, suggesting the potential utility of such results in some cases.

Several groups have used RPA and other amplification techniques, including loop-mediated isothermal amplification (LAMP) and rolling circle amplification (RCA), to facilitate rapid and simple diagnosis of mycobacteria from respiratory specimens, whereas others have used low-volume PCR to streamline the diagnostic workflow (*46*–*51*). However, most of these methods rely on separate DNA extraction methods, or other approaches, that are not suitable for use in resource-limited settings. For example, a WHO-supported LAMP assay uses an isothermal LAMP approach to rapidly amplify (<1 hour) an *Mtb* DNA target used for TB diagnosis but relies on a standard DNA isolation approach that limits its utility (*46*, *52*). Separate DNA isolation is also required by an RPA-based assay that sensitively detects and quantifies an *Mycobacterium smegmatis* DNA target using an electrochemical readout method (*48*) and an RCA-based assay reported to detect *rpoB* gene mutations associated with *Mtb* drug-resistant with high sensitivity and specificity (*49*). Last, low-volume droplet PCR assays have been used to detect *Mtb IS6110* at high sensitivity and may thus be particularly useful for TB diagnosis from saliva samples where Xpert reveals reduced sensitivity, but they rely on DNA isolation, as well as additional equipment that is not suitable for use in POC applications (*50*, *51*).

Downloaded from https://www.science.org at Tulane University on April 09, 2025

In contrast, in the LIT-TB approach described here, DNA concentration is achieved within the tube by lowering the device's inner plunger that holds a DNA capture membrane into a sputum or saliva specimen after a short, high-temperature incubation step has been used to inactivate and lyse any *Mtb* bacilli present in this sample. This plunger is then raised, twisted, and depressed again to bring an outer plunger holding a reagent-loaded membrane into contact with the DNA capture membrane to initiate the assay's RPA-CRISPR reaction. All of these steps, including the assay readout step, occur on the assay device without opening the assay tube, unlike previously described methods. Serum or plasma analyses differ in that cell-free DNA from these samples is isolated in a separate procedure and then applied to the DNA capture membrane before analysis using the remainder of the standard LIT-TB assay workflow.

Further analysis of TB bacilli and DNA loads in various sample types is needed before application of nonsputum diagnostics. Mean *Mtb* bacilli concentrations reported for sputum specimens range from 10^3 to 10^5 CFU/ml, although age, HIV status, sputum specimen quality, and other factors can influence these estimates, and these values do not directly reflect the amount of *Mtb* genomic DNA present in these samples, which should be higher because of the presence of nonviable *Mtb* bacilli (*53*, *54*). We could not find similar *Mtb* CFU/ml estimates for saliva, but at least one study that has analyzed both specimens with GeneXpert Ultra observed higher relative signals (78% versus 19% moderate/high) in sputum versus saliva samples from the same patients, although this study did not provide cycle threshold (Ct) values or other more quantitative results (*28*). Few studies have reported mean *Mtb* cfDNA concentrations detected in the sera of individuals with TB. We have previously reported that the mean *Mtb* cfDNA concentration detected in sera obtained from one cohort of young children with TB was 5.58 copies/μl, although about half the samples tested had *Mtb* cfDNA concentrations of <0.25 copies/μl, with a median concentration of 0.13 copies/μl (*24*). We could not find similar *Mtb* CFU/ml estimates for saliva, but at least one study that analyzed both specimens with GeneXpert Ultra observed higher relative signal (78% versus 19% moderate/high) in sputum versus saliva samples from the same patients, although this study did not provide Ct values or other more quantitative results (*28*).

Saliva and oral swab samples have been investigated as potential alternative specimens for TB diagnostics because they can be readily obtained from all patients, unlike other respiratory specimens (*27*, *55*, *56*), and because Xpert exhibits similar diagnostic performance when used to analyze saliva or sputum (*28*). *Mtb* DNA signals detected in saliva were lower and more variable than sputum signals, although matching samples were not available from a single cohort for direct comparison. Saliva-based LIT TB could thus have reduced performance for some patients with PTB, particularly those who have low *Mtb* concentrations in their respiratory specimens, although this might be mitigated by optimizing sample collection or analyzing serial specimens similar to Xpert assays. Nevertheless, these findings imply that a LIT system could analyze respiratory specimens at the POC in remote or resource-limited settings without access to Xpert to expand TB diagnostic efforts.

Normally, GeneXpert would be limited to sites with the resources to purchase and operate an Xpert system (a minimum of $19,000 per machine and approximately $8 per sample, with subsidies) (*57*, *58*), but our findings indicate that saliva and sputum LIT-TB assay results have good diagnostic performance for PTB at low cost (<$800 per instrument and $2.62 per sample). In addition, LIT-TB cost per machine is largely attributed to an expensive optics system ($690), which could be replaced with low-cost excitation and emission filters to substantially reduce cost at scale. Use of Xpert in resource-limited settings requires either that samples be shipped to a centralized laboratory or that an Xpert system, computer, power source, and other incidental materials be transported to the site and operated in an area with at least minimal environmental control, neither of which may be practical (*59*–*62*).

Further work should be performed to address the limitations of this study. For example, although saliva, sputum, and serum LIT-TB results all had strong diagnostic performance for PTB, it is not clear how these results correlate, particularly after treatment initiation. This assay also targeted a multicopy *Mtb* insertion element, *IS6110*, to increase detection sensitivity, but *IS6110* can be absent or present at variable copies in some *Mtb* strains to complicate diagnosis and the potential to estimate absolute *Mtb* burden. However, given the strong LIT-TB signal detected in most analyzed specimen types, it should be possible to instead use conserved single-copy *Mtb*-specific DNA sequences to address this issue. Although our assay did not meet the minimum storage requirements of the WHO TPP for TB diagnosis by POC assays (12 months at +5°C to +35°C with up to 70% humidity), it may be possible to achieve the targeted stability by optimizing the reagent lyophilization conditions using excipients that stabilize RPA and Cas12a enzyme activity during and after this process. Last, although serum-based LIT-TB results can diagnose both PTB and EPTB, unlike results from saliva and sputum, and may be superior to these samples in young children and individuals with compromised immune responses, they also require venipuncture, serum collection, and cell-free DNA isolation that prevents direct analysis by the LIT-TB assay system. However, all of these procedures can be readily performed in resource-limited settings, and it may be possible to use fingerstick blood samples and microfluidic plasma and DNA isolation procedures to streamline this process. Thus, LIT-TB results from both respiratory and serum/plasma specimens may have value in improving TB screening in areas with high disease burden and limited resources.

MATERIALS AND METHODS

Study design

The objective of this study was to develop and validate the performance of a POC LIT-TB diagnostic system intended to fulfill the criteria proposed by the WHO for new TB diagnostics that evaluate nonsputum specimens, using serum and saliva, and evaluate its performance against reference sputum-based tests when used to analyze sputum specimens. A secondary objective of this study was to evaluate how LIT-TB results obtained with longitudinal serum samples of individuals diagnosed with TB changed with anti-TB treatment duration. No sample size analysis was performed for this study, which analyzed all available samples from cryopreserved sample archives of retrospective study cohorts. All LIT-TB analyses were performed by operators blinded to all clinical and demographic information associated with these samples. Specimens were collected only after the study participants or their legal guardians gave informed consent or assent that their samples and anonymized clinical results could be used for future research. LIT-TB results from serum, saliva, and sputum specimens represent the values obtained from a single analysis of each sample.

Downloaded from https://www.science.org at Tulane University on April 09, 2025

Serum specimens were collected from children in the Dominican Republic who were aged ≤18 years and diagnosed with TB using a research protocol approved by the Human Subjects Institutional Review Board at the University of Miami and the O&M School of Medicine, Santo Domingo, the Dominican Republic (protocol nos. 20180453 and 00010285). Serum specimens analyzed in this study were derived from children with bacteriologic confirmation of TB (confirmed TB) by positive culture or GeneXpert results or clinical confirmation of TB (unconfirmed TB) by least two of the following criteria: (i) symptoms suggestive of TB, (ii) a chest radiograph consistent with TB, (iii) close TB exposure or immunological evidence of *Mtb* infection, or (iv) a positive response to antimicrobial treatment for TB. Effective response to anti-TB treatment was defined as resolution of all presenting signs and symptoms consistent with TB (as defined in the 2015 National Institutes of Health consensus definition for intrathoracic TB in children) at the last scheduled study visit, which predominantly occurred 24 weeks after the study entry. Standard sputum samples were directly obtained from all children who were able to expectorate normally. Nebulization or gastric lavage was used to induce sputum production or directly obtain respiratory specimens from children who could not voluntarily produce sputum. Nebulization was used to obtain sputum if a child was >4 years old and could not naturally produce sputum, and gastric lavage was used to obtain respiratory specimens in children <4 years old. Sera were also obtained from children (<18 years) in New Orleans, Louisiana who had low likelihood of TB after obtaining their parent's or guardian's consent using an institutional review board–approved protocol (protocol no. 2020-493).

Saliva samples were collected from participants who gave consent for these specimens to be used for future TB research using a protocol approved by the institutional review board at University of California, San Diego (protocol no. 190917) and by the ethics committees of each field site: Universidad Autonoma de Nuevo Leon Comite de Etica en Investigacion (reference no. NM20-00018) and the National Bioethics Committee of Pakistan (reference no. 4-87/ NBC-595/21/ 1367). Specimens analyzed in this study were obtained from individuals who were classified as having TB by positive culture or Xpert results obtained upon analysis of their sputum specimens or who lacked evidence of *Mtb* infection as determined by a negative QuantiFERON-TB Gold Test results.

Raw deidentified sputum specimens were obtained through a Houston Methodist Research Institute collaboration with the City of Houston Mycobacterial Laboratory (institutional review board no. CR00000563). All sputum specimens were obtained in the morning, with most individuals providing specimens on three consecutive mornings. In most situations, 3 to 10 ml of the sputa and or respiratory fluid was recovered for solid (Lowenstein Jenson) and liquid (mycobacterial growth indicator tube) culture and smear analyses used for TB diagnosis. Before the concentration procedure, a 1- to 2-ml aliquot of each specimen was aliquoted into two 1.5-ml screw-tops O-rings cryotubes, which were assigned a study number and stored at −80°C until analysis.

Standard and membrane-based RPA-CRISPR reactions

RPA reaction cocktails were generated by adding 13.2 μl of water, 2.4 μl of 10 μM forward primer, 2.4 μl of 10 μM reverse primer, 5% sucrose (w/v), and 29.5 μl of primer-free rehydration buffer (TwistDx, TABAS03KIT) to an RPA pellet. CRISPR reaction cocktails were generated by adding 640 μl of water, 4 μl of 100 μM fluorescent reporter, 0.4 μl of 100 μM gRNA, and 0.4 μl of EnGen Lba Cas12a (100 μM; New England Biolabs). RPA-CRISPR reactions were generated by mixing 15 μl of RPA reaction cocktail, 8 μl of CRISPR reaction cocktail, and 2 μl of MgOAc and then adding 5 μl of a DNA template solution or 5 μl of water for nontemplate control reactions. Reactions analyzed by a plate reader were quantified using a Tecan Infinite M Plex plate reader. Reaction kinetic studies were performed using 25°, 30°, 37°, and 42°C incubation temperatures. In lyophilization studies, 30 μl of the RPA-CRISPR reaction mixture was added to 3-mm discs of cotton blot paper (Bio-Rad, 1703969), nitrocellulose or Whatman 3, 4, 113, or 541 membranes (Whatman 10401106,1003-323, 1004-04, 11113-110, and 1541-042), and PES membrane (MilliporeSigma, GPWP02500). Reagent-loaded membranes were then flash-frozen with liquid nitrogen and lyophilized overnight using a VirTis 25EL lyophilizer. Reagent-loaded membranes were then either rehydrated with a template DNA solution and analyzed for RPA-CRISPR signal production over a 3-hour interval using a fluorescent plate reader or stored under vacuum in black food saver bags (Shield N Seal SNS 1700) with desiccant at −20°, 4°, or 23°C until evaluated for stability during long-term storage at the indicated temperatures. Reactions that analyzed membrane fluorescence background on reagent-loaded membranes (fig. S1A) were imaged using a Bio-Rad ChemiDoc imaging system, and quantitative values for the Cy5 and fluorescein amidite (FAM) signal of these membranes were analyzed using ImageJ with the signal-to-noise ratio calculated by dividing the fluorescence detected after a 15-min incubation at 37°C by the fluorescence at baseline.

Spike-in samples and DNA standards

DNA standards consisting of *Mtb* genomic DNA and plasmids were prepared for spike-in sample analysis. *Mtb* genomic DNA standards were prepared from irradiation-sterilized *Mtb* H37Ra bacilli aliquots (BEI Resources, NR-122) using a DNeasy blood and tissue kit (QIAGEN, 69506), and genomic DNA from *Mycobacterium kansasii*, *Mycobacterium abscessus*, *Mycobacterium avium*, and *Mycobacterium intracellulare* was obtained from the American Type Culture Collection (12478, 19977, BAA-968, and 35774). *Mtb* genomic DNA was diluted and spiked into healthy human serum (Sigma-Aldrich, H4522), artificial sputum (Claremont Bio, 01.384.25), normal human saliva (BioIVT), or nuclease-free water for specific analyses. An *IS6110* sequence region amplified from *Mtb* genomic DNA was cloned into a TOPO vector and transformed into *Escherichia coli* cells (TOPO TA cloning kits, K4500-01SC), and recombinant *IS6110* plasmid DNA was isolated from cultured bacterial clones with a Zyppy plasmid miniprep kit (Zymo Research, D4019), quantified using the Qubit dsDNA high sensitivity assay kit (Invitrogen Q32851), and diluted into artificial sputum. Spike-in H37Rv standard for LoD analysis was created by spiking H37Rv (10,000 CFU/ml; ZeptoMetrix, 0801661) into artificial sputum and creating 2× serial dilutions. Standard curve for estimation of LoD in copies/μl was conducted using a two-pot CRISPR-TB assay targeting the *IS6110* plasmid. For this assay, 5 μl of plasmid was mixed with 12.5 μl of 2x Magic Green Taq Supermix (ToloBio, no. 21502-C), 1.25 μl of forward primer, 1.25 μl of reverse primer, and 5 μl of nuclease-free water. PCR reactions were performed according to the following protocol: 94°C for 2 min, 38 cycles of (98°C for 10 s, 60°C for 10 s, and 72°C for 15 s), and 72°C for 5 min. Two microliters of the PCR reaction was mixed with 30 μl of CRISPR reagents [25.48 μl of nuclease-free water, 0.01 μl of 66.7 μM IDT LbCas12a (Integrated

Downloaded from https://www.science.org at Tulane University on April 09, 2025

DNA Technologies, 10007922), 0.01 μl of 100 μM gRNA, 1.5 μl of 10 μM fluorescent reporter, and 3 μl of NEBuffer 2.1 (New England Biolabs, B7202)]. CRISPR reactions were incubated at 37°C for 15 min in the dark in a 96-well Corning half area opaque plate, and fluorescence was read by an Infinite M Plex (Tecan) plate reader.

Respiratory sample liquification, lysis, and DNA capture optimization

Saliva liquification conditions were analyzed using human saliva samples spiked to achieve 10 mM DTT, 5 mM EGTA (MilliporeSigma, E4378-10G), 5 mM tris(2-carboxyethyl) phosphine (Thermo Fisher Scientific, 77720), 1 mM EDTA concentrations, or one-to-one ratios with QuickExtract RNA or DNA extraction solution (Biosearch Technologies, SS000880-D2 and SS000035-D2) or one-to-one ratios with DNA/RNA shield (Zymo Research, R1100), incubated at RT for 10 min, and evaluated for pre- to posttreatment 600-nm absorbance changes with a SpectraMax iD5 (Molecular Devices) spectrophotometer. Sputum liquification conditions were analyzed using artificial and human sputum samples spiked to achieve 100 or 1000 mM DTT or 2% NaOH concentrations or one-to-two sputum-to-isopropanol ratios, incubated at RT for 10 min, and evaluated as described above. The optimum temperature requirement for DNA release from intact *Mtb* bacilli was evaluated by spiking irradiation-sterilized *Mtb* H37Ra bacilli into artificial sputum samples that were incubated at 25°, 45°, 65°, and 95°C for 10 min after liquification with 100 mM DTT and then analyzing the RTA-CRISPR *Mtb* signals produced when 5-μl aliquots of these samples were added to RPA-CRISPR reagent–loaded paper strips that were incubated at 37°C for 45 min and then analyzed for Cy5 signal by a fluorescent plate reader. In the membrane-based DNA enrichment analyses, heat-treated, DTT-liquified *Mtb*-spiked artificial sputum samples were added to small discs of PES (MilliporeSigma, GPWP02500), Whatman 1 (Whatman, 1001-042), 0.2- and 5-μm polycarbonate (MilliporeSigma, GTTP02500 and TMTP04700), cotton blot (Bio-Rad, 1703969), and cotton grade 222 (Ahlstrom, 2228-1616) membranes; then washed with 10 mM (pH 8) tris buffer; laid atop RPA-CRISPR reagent–loaded paper; incubated at 37°C for 45 min; and read by a fluorescent plate reader.

H37Rv heat sterilization experiment

All steps of the *Mtb* H37Rv heat sterilization experiment were conducted in the Biosafety Level 3 lab at the Tulane National Primate Research Center. Briefly, *Mtb* H37Rv (ZeptoMetrix, 0801661) was cultured in 7H9 medium until log-phase growth (optical density, 0.4), transferred to a conical tube, and centrifuged for 10 min, after which the supernatant was aspirated, and the pellet was resuspended in artificial sputum. Five hundred–microliter aliquots of these spiked sputum samples were heated at 80°C for 15 or 30 min in a heat block (Benchmark Scientific, H500-5), and 100 μl of these heat-treated samples was plated onto 7H11 agar plates, cultured for 4 weeks at 37°C, and evaluated for colony formation. A serial dilution series of *Mtb* H37Rv samples was also spiked into artificial sputum to estimate the concentration of *Mtb* H37Rv in the log-phase culture. Briefly, an aliquot of this culture was serially diluted in artificial sputum to generate six 10-fold dilution samples, which were then cultured for 4 weeks at 37°C on 7H11 agar plates. After 4 weeks, individual colonies that formed on these plates were used to estimate the CFU/ml concentration by multiplying the mean number of colonies detected on a set of triplicate cultures for each dilution sample by the dilution factor of the sample added to these plates.

Construction of the LIT assay incubator and reader

A 3D-printed case for the handheld assay device was fitted with a rechargeable battery, a miniature incubator, imaging components, a 3.5-inch (8.89 cm) touchscreen, and a Raspberry Pi microprocessor (table S1). A custom microincubator was fabricated from a heating element (Amazon, B0727X2DGC) and insulation was fitted to the shape of the assay tube. To determine the best insulation material for the assay incubator component of the handheld assay device, we recorded temperature differentials (ΔT) and the corresponding durations (t) for these changes and determined the theoretical heating time ($t_{\text{theoretical}}$) necessary to elevate the temperature of a fixed volume of water (1 ml) under prescribed power output conditions (1 W) for the given ΔT when this tube was surrounded by pine wood, Styrofoam, polyethylene packing material, or no isolation. We then calculated percent efficiency (η) of the heating process using the equation: $\eta = (t_{\text{theoretical}}/t) \times 100$ for each material. The temperature profile assay tubes held in the incubator port of this device were mapped by replacing the LIT plunger with a thermocouple and measuring the temperature gradient from the bottom to the top of these tubes to identify the region corresponding to the optimum RPA-CRISPR reaction temperature range.

The optical imaging module of this device was produced by aligning a laser diode (Amazon, B08R9XBVM3) with a filter cube containing an excitation filter (Edmond Optics, 67-035), a dichroic mirror (Edmond Optics, 67-084), and an emission filter (Edmond Optics, 67-038) positioned adjacent to the camera (PiShop, 46-1). A microprocessor (PiShop, Pi3B), powered by a rechargeable battery (Amazon, B08T8TDS8S), controlled the light source and the camera during image acquisition, and results were then displayed on a 3.5-inch (8.89 cm) liquid crystal display (LCD) touchscreen interface (Waveshare, 9904) for user interactions. Camera control and image analysis were regulated by using an algorithm written in Python (version 3.10) using the Picamera2 library (version 0.3.16) to regulate the RPi camera module 3 image capture parameters, using a fixed 10-cm imaging distance and 10-s exposure time and augmenting the analog gain to enhance image quality. Image analyses were performed using OpenCV (version 4.8.1.78) by isolating the red channel, applying a Gaussian blur (three-by-three kernel size) to eliminate noise, delineating a circle around the target region with the correct radius, generating a mask for the intensity calculation, and computing average and SD values. Text annotations were strategically placed on the image, and the final processed image was displayed to the user through the LCD screen.

The ROI for signal quantification was defined by refining the diameter of a circular region corresponding to the position of the assay reagents and centered on the geometric midpoint of the laser focus determined by the fixed position of the optical components, with all signal detected outside this region treated as noise to minimize potential interference. This optimization calculated the noise in images captured for three negative controls and then determined an acceptable noise threshold by ensuring at least 95% of the pixels within defined circle reflected true signal when analyzing positive control samples. This process was iteratively applied across a range of radii, culminating in the selection of the radius generating the most favorable signal-to-noise ratio for subsequent analyses.

Downloaded from https://www.science.org at Tulane University on April 09, 2025

LIT assay tube design and use

The LIT assay tube design uses a 5-ml round-bottom polypropylene tube (Globe Scientific, 110446) fitted with a 3D-printed plunger that contains a 6-mm PES/Whatman DNA enrichment membrane, placed below a cotton blot membrane disc loaded with RPA-CRISPR reagents. The 3D-printed plunger is composed of five separate 3D-printed parts and two identical rubber bands (Amazon, B08B3K2RBS) that, when assembled and inserted into the polypropylene tube, form a closed system. This plunger uses a pen click mechanism to control its movement within the sealed chamber, where the first click of the plunger lowers its DNA capture membrane into the sample lysate and the second click raises this membrane and brings it into contact with a membrane containing RPA-CRISPR reagents to initiate the reaction used to detect the target DNA fragment.

For saliva and sputum analyses, 500 μl of patient respiratory sample was added to two distinct LIT assay tube variants containing lyophilized DTT amounts designed to achieve 10 or 100 mM DTT final concentrations in these respective sample types, which were transferred to the incubator port of the portable assay device for 15 min to permit *Mtb* lysis and deoxyribonuclease (DNase) inactivation. After 7 min, tubes were removed and shaken briefly, replaced, and allowed to incubate for an additional 8 min, after which their plungers were depressed to lower the DNA enrichment membrane into the sample lysate by the 3D-printed clicker, and then a second click orchestrates contact onto reagent-loaded blot paper to initiate the RPA-CRISPR reaction within the 37°-to-42°C region of the assay tube. For pediatric serum analyses, DNA was isolated from 200 μl of serum samples using a MagMAX cell-free DNA isolation kit (Applied Biosystems, A29319) on a KingFisher Flex (Thermo Fisher Scientific) system, eluted in 50 μl of DNase-free water, and stored at −80°C until use. A 5-μl aliquot (10%) of a sample was added directly to the RPA-CRISPR detection membrane and incubated for 45 min in a LIT assay tube loaded with 1 ml of phosphate-buffered saline to generate the standard 37° to 42°C region in the assay tube. After the RPA-CRISPR reaction, the LIT assay tubes were transferred to the assay readout port to quantify assay signal by selecting the OpenCV icon using the device touchscreen to capture a fluorescent image and calculate a quantitative result, both of which are automatically displayed on the touchscreen. The positive signal cutoff value was calculated as the mean plus three times the SD value detected from three independent no template control assay reactions. The assay value can be recorded by hand or saved on the microprocessor and exported to another device using the Universal Serial Bus (USB) port or Bluetooth or WiFi functions of the microprocessor.

Statistical analysis

Total fluorescent values are reported for all experiments except for the temperature kinetic study that reported background-subtracted fluorescent values (fluorescence subtracted by fluorescence at time zero). GraphPad Prism 8 was used to visualize data and calculate linear regression of the standard curve, and differences between groups were analyzed by Kruskal-Wallis tests with Dunn's posttests for multiple comparisons, Welch analysis of variance (ANOVA) with Dunnett's T3 for multiple comparisons, or Welch's *t* test (unpaired and does not assume equal SDs), as indicated in the text. Comparisons made with Kruskal-Wallis tests assumed that the variable being analyzed was ordinal or continuous and that the groups being compared were independent and derived from populations with the same distribution, whereas those performed with Welch's *t* tests assumed that both groups were sampled from populations with normal distributions. Comparisons made with Welch ANOVAs assumed that the groups being compared had normal distributions and that their SDs were unequal. Differences were considered statistically significant at $P < 0.05$. CIs for diagnostic sensitivity estimates were determined by the Clopper-Pearson exact method by MedCalc (https://medcalc.org/calc/diagnostic_test.php), whereas those for data distribution were calculated using the sample mean, SD, and population size using the CONFIDENCE.NORM function of Excel. All sample sizes are presented in the figure legends. All individual-level data are available in data file S2.

Supplementary Materials

The PDF file includes:

Figs. S1 to S22
Tables S1 to S7
References (*63*–*68*)

Other Supplementary Material for this manuscript includes the following:

Data files S1 and S2
Movie S1
MDAR Reproducibility Checklist

REFERENCES AND NOTES

1. G. J. Abou Jaoude, I. Garcia Baena, P. Nguhiu, A. Siroka, T. Palmer, L. Goscé, K. Allel, E. Sinanovic, J. Skordis, H. Haghparast-Bidgoli, National tuberculosis spending efficiency and its associated factors in 121 low-income and middle-income countries, 2010–19: A data envelopment and stochastic frontier analysis. *Lancet Global Health* **10**, e649–e660 (2022).
2. WHO, "Global Tuberculosis Report 2022" (2022).
3. WHO, "The END TB Strategy" (2015).
4. A. Esmail, P. Randall, S. Oelofse, M. Tomasicchio, A. Pooran, R. Meldau, E. Makambwa, L. Mottay, S. Jaumdally, G. Calligaro, S. Meier, M. De Kock, T. Gumbo, R. M. Warren, K. Dheda, Comparison of two diagnostic intervention packages for community-based active case finding for tuberculosis: An open-label randomized controlled trial. *Nat. Med.* **29**, 1009–1016 (2023).
5. G. Zwama, K. Diaconu, A. S. Voce, F. O'May, A. D. Grant, K. Kielmann, Health system influences on the implementation of tuberculosis infection prevention and control at health facilities in low-income and middle-income countries: A scoping review. *BMJ Glob. Health* **6**, e004735 (2021).
6. M. Nadjib, R. K. Dewi, E. Setiawan, T. Y. Miko, S. Putri, P. F. Hadisoemarto, E. R. Sari, Pujiyanto, R. Martina, L. N. Syamsi, Cost and affordability of scaling up tuberculosis diagnosis using Xpert MTB/RIF testing in West Java, Indonesia. *PLOS ONE* **17**, e0264912 (2022).
7. A. S. Piatek, M. Van Cleeff, H. Alexander, W. L. Coggin, M. Rehr, S. Van Kampen, T. M. Shinnick, Y. Mukadi, GeneXpert for TB diagnosis: Planned and purposeful implementation. *Glob. Health Sci. Pract.* **1**, 18–23 (2013).
8. WHO, "Xpert MTB/RIF Implementation Manual Technical and Operational 'How-to': Practical Considerations" (2014).
9. R. Vongthilath-Moeung, A. Poncet, G. Renzi, J. Schrenzel, J.-P. Janssens, Time to detection of growth for *Mycobacterium tuberculosis* in a low incidence area. *Front. Cell. Infect. Microbiol.* **11**, 704169 (2021).
10. M. D. Fenta, O. A. Ogundijo, A. A. A. Warsame, A. G. Belay, Facilitators and barriers to tuberculosis active case findings in low- and middle-income countries: A systematic review of qualitative research. *BMC Infect. Dis.* **23**, 515 (2023).
11. WHO, "High-Priority Target Product Profiles for New Tuberculosis Diagnostics: Report of a Consensus Meeting" (2014).
12. H. Alsdurf, B. Empringham, C. Miller, A. Zwerling, Tuberculosis screening costs and cost-effectiveness in high-risk groups: A systematic review. *BMC Infect. Dis.* **21**, 935 (2021).
13. J. Y. Lee, Diagnosis and treatment of extrapulmonary tuberculosis. *Tuberc. Respir. Dis.* **78**, 47–55 (2015).
14. R. Gopalaswamy, V. N. A. Dusthackeer, S. Kannayan, S. Subbian, Extrapulmonary tuberculosis—An update on the diagnosis, treatment and drug resistance. *J. Respir.* **1**, 141–164 (2021).
15. T. A. Thomas, Tuberculosis in children. *Pediatr. Clin. North Am.* **64**, 893–909 (2017).

Downloaded from https://www.science.org at Tulane University on April 09, 2025

16. R. K. Gupta, S. B. Lucas, K. L. Fielding, S. D. Lawn, Prevalence of tuberculosis in post-mortem studies of HIV-infected adults and children in resource-limited settings. *AIDS* **29**, 1987–2002 (2015).
17. T. G. Connell, H. J. Zar, M. P. Nicol, Advances in the diagnosis of pulmonary tuberculosis in HIV-infected and HIV-uninfected children. *J. Infect. Dis.* **204**, S1151–S1158 (2011).
18. H. E. Jenkins, C. M. Yuen, C. A. Rodriguez, R. R. Nathavitharana, M. M. McLaughlin, P. Donald, B. J. Marais, M. C. Becerra, Mortality in children diagnosed with tuberculosis: A systematic review and meta-analysis. *Lancet Infect. Dis.* **17**, 285–295 (2017).
19. M. T. Montales, A. Chaudhury, A. Beebe, S. Patil, N. Patil, HIV-associated TB syndemic: A growing clinical challenge worldwide. *Front. Public Health* **3**, 281 (2015).
20. S.-A. Ohene, M. I. Bakker, J. Ojo, A. Toonstra, D. Awudi, P. Klatser, Extra-pulmonary tuberculosis: A retrospective study of patients in Accra, Ghana. *PLOS ONE* **14**, e0209650 (2019).
21. I. Bouzouita, A. Ghariani, K. B. Dhaou, S. Jemaeil, L. Essaalah, S. Bejaoui, H. Draoui, N. El Marzouk, E. Mehiri, L. Slim-Saidi, Usefulness of Xpert MTB/RIF Ultra for rapid diagnosis of extrapulmonary tuberculosis in Tunisia. *Sci. Rep.* **14**, 2217 (2024).
22. M. Tadesse, G. Abebe, A. Bekele, M. Bezabih, D. Yilma, L. Apers, B. C. De Jong, L. Rigouts, Xpert MTB/RIF assay for the diagnosis of extrapulmonary tuberculosis: A diagnostic evaluation study. *Clin. Microbiol. Infect.* **25**, 1000–1005 (2019).
23. E. Maclean, T. Broger, S. Yerlikaya, B. L. Fernandez-Carballo, M. Pai, C. M. Denkinger, A systematic review of biomarkers to detect active tuberculosis. *Nat. Microbiol.* **4**, 748–758 (2019).
24. Z. Huang, S. M. LaCourse, A. W. Kay, J. Stern, J. N. Escudero, B. M. Youngquist, W. Zheng, D. Vambe, M. Dlamini, G. Mtetwa, L. M. Cranmer, I. Njuguna, D. C. Wamalwa, E. Maleche-Obimbo, D. G. Catanzaro, C. J. Lyon, G. John-Stewart, A. DiNardo, A. M. Mandalakas, B. Ning, T. Y. Hu, CRISPR detection of circulating cell-free *Mycobacterium tuberculosis* DNA in adults and children, including children with HIV: A molecular diagnostics study. *Lancet Microbe* **3**, E482–E492 (2022).
25. S. G. Thakku, J. Lirette, K. Murugesan, J. Chen, G. Theron, N. Banaei, P. C. Blainey, J. Gomez, S. Y. Wong, D. T. Hung, Genome-wide tiled detection of circulating *Mycobacterium tuberculosis* cell-free DNA using Cas13. *Nat. Commun.* **14**, 1803 (2023).
26. R. C. Wood, A. K. Luabeya, K. M. Weigel, A. K. Wilbur, L. Jones-Engel, M. Hatherill, G. A. Cangelosi, Detection of *Mycobacterium tuberculosis* DNA on the oral mucosa of tuberculosis patients. *Sci. Rep.* **5**, 8668 (2015).
27. E. C. Church, K. R. Steingart, G. A. Cangelosi, M. Ruhwald, M. Kohli, A. E. Shapiro, Oral swabs with a rapid molecular diagnostic test for pulmonary tuberculosis in adults and children: A systematic review. *Lancet Glob. Health* **12**, e45–e54 (2024).
28. P. Byanyima, S. Kaswabuli, E. Musisi, C. Nabakiibi, J. Zawedde, I. Sanyu, A. Sessolo, A. Andama, W. Worodria, L. Huang, J. L. Davis, R. Wood, Feasibility and sensitivity of saliva GeneXpert MTB/RIF ultra for tuberculosis diagnosis in adults in Uganda. *Microbiol. Spectrum* **10**, e0086022 (2022).
29. K. J. Land, D. I. Boeras, X. S. Chen, A. R. Ramsay, R. W. Peeling, REASSURED diagnostics to inform disease control strategies, strengthen health systems and improve patient outcomes. *Nat. Microbiol.* **4**, 46–54 (2019).
30. P. Ma, T. Luo, L. Ge, Z. Chen, X. Wang, R. Zhao, W. Liao, L. Bao, Compensatory effects of *M. tuberculosis rpoB* mutations outside the rifampicin resistance-determining region. *Emerg. Microbes Infect.* **10**, 743–752 (2021).
31. M.-C. Li, X.-Y. Wang, T.-Y. Xiao, S.-Q. Lin, H.-C. Liu, C. Qian, D. Xu, G.-L. Li, X.-Q. Zhao, Z.-G. Liu, L.-L. Zhao, K.-L. Wan, *rpoB* Mutations are associated with variable levels of rifampin and rifabutin resistance in *Mycobacterium tuberculosis*. *Infect. Drug Resist.* **15**, 6853–6861 (2022).
32. D. R. Joel, A. P. Steenhoff, P. C. Mullan, B. R. Phelps, M. A. Tolle, A. Ho-Foster, V. Mabikwa, B. G. Kgathi, R. Ncube, G. M. Anabwani, Diagnosis of paediatric tuberculosis using sputum induction in Botswana: Programme description and findings. *Int. J. Tuberc. Lung Dis.* **18**, 328–334 (2014).
33. B. J. Marais, H. S. Schaaf, Childhood tuberculosis: An emerging and previously neglected problem. *Infect. Dis. Clin. North Am.* **24**, 727–749 (2010).
34. J. G. Peter, G. Theron, N. Singh, A. Singh, K. Dheda, Sputum induction to aid diagnosis of smear-negative or sputum-scarce tuberculosis in adults in HIV-endemic settings. *Eur. Respir. J.* **43**, 185–194 (2014).
35. C. Doig, A. L. Seagar, B. Watt, K. J. Forbes, The efficacy of the heat killing of *Mycobacterium tuberculosis*. *J. Clin. Pathol.* **55**, 778–779 (2002).
36. P. Shetty, D. Ghosh, D. Paul, Thermal lysis and isothermal amplification of *Mycobacterium tuberculosis* H37Rv in one tube. *J. Microbiol. Methods* **143**, 1–5 (2017).
37. P. Bemer-Melchior, H. B. Drugeon, Inactivation of *Mycobacterium tuberculosis* for DNA typing analysis. *J. Clin. Microbiol.* **37**, 2350–2351 (1999).
38. H. de Puig, R. A. Lee, D. Najjar, X. Tan, L. R. Soekensen, N. M. Angenent-Mari, N. M. Donghia, N. E. Weckman, A. Ory, C. F. Ng, P. Q. Nguyen, A. S. Mao, T. C. Ferrante, G. Lansberry, H. Sallum, J. Niemi, J. J. Collins, Minimally instrumented SHERLOCK (miSHERLOCK) for CRISPR-based point-of-care diagnosis of SARS-CoV-2 and emerging variants. *Sci. Adv.* **7**, eabh2944 (2021).
39. Y. Zou, M. G. Mason, Y. Wang, E. Wee, C. Turni, P. J. Blackall, M. Trau, J. R. Botella, Nucleic acid purification from plants, animals and microbes in under 30 seconds. *PLOS Biol.* **15**, e2003916 (2017).
40. Y. Chen, Y. Hu, X. Lu, Polyethersulfone-based microfluidic device integrated with DNA extraction on paper and recombinase polymerase amplification for the detection of *Salmonella enterica*. *ACS Sens.* **8**, 2331–2339 (2023).
41. D. Helb, M. Jones, E. Story, C. Boehme, E. Wallace, K. Ho, J. Kop, M. R. Owens, R. Rodgers, P. Banada, H. Safi, R. Blakemore, N. T. N. Lan, E. C. Jones-López, M. Levi, M. Burday, I. Ayakaka, R. D. Mugerwa, B. McMillan, E. Winn-Deen, L. Christel, P. Dailey, M. D. Perkins, D. H. Persing, D. Alland, Rapid detection of *Mycobacterium tuberculosis* and rifampin resistance by use of on-demand, near-patient technology. *J. Clin. Microbiol.* **48**, 229–237 (2010).
42. Y. He, C. J. Lyon, D. T. Nguyen, C. Liu, W. Sha, E. A. Graviss, T. Y. Hu, Serum-based diagnosis of pediatric tuberculosis by assay of *Mycobacterium tuberculosis* factors: A retrospective cohort study. *J. Clin. Microbiol.* **59**, e0175620 (2021).
43. S.-W. Pan, W.-J. Su, Y.-J. Chan, F.-Y. Chuang, J.-Y. Feng, Y.-M. Chen, Mycobacterium tuberculosis–derived circulating cell-free DNA in patients with pulmonary tuberculosis and persons with latent tuberculosis infection. *PLOS ONE* **16**, e0253879 (2021).
44. G. Theron, R. Venter, G. Calligaro, L. Smith, J. Limberis, R. Meldau, D. Chanda, A. Esmail, J. Peter, K. Dheda, Xpert MTB/RIF results in patients with previous tuberculosis: Can we distinguish true from false positive results? *Clin. Infect. Dis.* **62**, 995–1001 (2016).
45. G. Theron, R. Venter, L. Smith, A. Esmail, P. Randall, V. Sood, S. Oelfese, G. Calligaro, R. Warren, K. Dheda, False-positive Xpert MTB/RIF results in retested patients with previous tuberculosis: Frequency, profile, and prospective clinical outcomes. *J. Clin. Microbiol.* **56**, e0169617 (2018).
46. WHO, "The Use of Loop-Mediated Isothermal Amplification (TB-LAMP) for the Diagnosis of Pulmonary Tuberculosis: Policy Guidance" (2016).
47. D. S. Boyle, R. McNerney, H. Teng Low, B. T. Leader, A. C. Pérez-Osorio, J. C. Meyer, D. M. O'Sullivan, D. G. Brooks, O. Piepenburg, M. S. Forrest, Rapid detection of *Mycobacterium tuberculosis* by recombinase polymerase amplification. *PLOS ONE* **9**, e103091 (2014).
48. M. N. Tsaloglou, A. Nemiroski, G. Camci-Unal, D. C. Christodouleas, L. P. Murray, J. T. Connelly, G. M. Whitesides, Handheld isothermal amplification and electrochemical detection of DNA in resource-limited settings. *Anal. Biochem.* **543**, 116–121 (2018).
49. X. Chen, B. Wang, W. Yang, F. Kong, C. Li, Z. Sun, P. Jelfs, G. L. Gilbert, Rolling circle amplification for direct detection of rpoB gene mutations in *Mycobacterium tuberculosis* isolates from clinical specimens. *J. Clin. Microbiol.* **52**, 1540–1548 (2014).
50. J. Yang, X. Han, A. Liu, X. Bai, C. Xu, F. Bao, S. Feng, L. Tao, M. Ma, Y. Peng, Use of digital droplet PCR to detect *Mycobacterium tuberculosis* DNA in whole blood-derived DNA samples from patients with pulmonary and extrapulmonary tuberculosis. *Front. Cell. Infect. Microbiol.* **7**, 369 (2017).
51. R. Ushio, M. Yamamoto, K. Nakashima, H. Watanabe, K. Nagai, Y. Shibata, K. Tashiro, T. Tsukahara, H. Nagakura, N. Horita, T. Sato, M. Shinkai, M. Kudo, A. Ueda, T. Kaneko, Digital PCR assay detection of circulating *Mycobacterium tuberculosis* DNA in pulmonary tuberculosis patient plasma. *Tuberculosis* **99**, 47–53 (2016).
52. C.-K. Kim, E. A. Cho, D. M. Shin, S. W. Choi, S. Y. Shin, Comparative evaluation of the loop-mediated isothermal amplification assay for detecting pulmonary tuberculosis. *Ann. Lab. Med.* **38**, 119–124 (2018).
53. M. Palaci, R. Dietze, D. J. Hadad, F. K. C. Ribeiro, R. L. Peres, S. A. Vinhas, E. L. N. Maciel, V. do Valle Dettoni, L. Horter, W. H. Boom, J. L. Johnson, K. D. Eisenach, Cavitary disease and quantitative sputum bacillary load in cases of pulmonary tuberculosis. *J. Clin. Microbiol.* **45**, 4064–4066 (2007).
54. E. Musisi, S. Wamutu, W. Ssengooba, S. Kasiinga, A. Sessolo, I. Sanyu, S. Kaswabuli, J. Zawedde, P. Byanyima, P. Kia, W. Muwambi, D. T. Toskin, E. Kigozi, N. Walbaum, E. Dombay, M. B. Legrady, K. D. Ssemambo, M. Joloba, D. Kuchaka, W. Worodria, L. Huang, S. H. Gillespie, W. Sabiiti, Accuracy of the tuberculosis molecular bacterial load assay to diagnose and monitor response to anti-tuberculosis therapy: A longitudinal comparative study with standard-of-care smear microscopy, Xpert MTB/RIF Ultra, and culture in Uganda. *Lancet Microbe* **5**, E345–E354 (2024).
55. A. R. Namuganga, N. N. Chegou, P. Mubiri, G. Walzl, H. Mayanja-Kizza, Suitability of saliva for tuberculosis diagnosis: Comparing with serum. *BMC Infect. Dis.* **17**, 600 (2017).
56. C. S. Laxton, C. Peno, A. M. Hahn, O. M. Allicock, S. Perniciaro, A. L. Wyllie, The potential of saliva as an accessible and sensitive sample type for the detection of respiratory pathogens and host immunity. *Lancet Microbe* **4**, E837–E850 (2023).
57. A. W. Kaso, A. Hailu, Costs and cost-effectiveness of Gene Xpert compared to smear microscopy for the diagnosis of pulmonary tuberculosis using real-world data from Arsi zone, Ethiopia. *PLOS ONE* **16**, e0259056 (2021).
58. The Global Fund, "Briefing Note New Pricing for Cepheid GeneXpert Tuberculosis Testing" (2023).
59. W. A. Alemayehu, S. Neri, S. Dalebout, R. Nalikungwi, A. Trusov, E. Ahmed, A. Dimba, A. Weirich, P. S. Curry, C. D. Kelly-Cirino, Comparative study of OMNIgene®•SPUTUM

Downloaded from https://www.science.org at Tulane University on April 09, 2025

reagent versus cold-chain for the transportation of sputum samples to GeneXpert®MTB/RIF testing sites in Malawi. *BMC Infect. Dis.* **19**, 424 (2019).
60. S. Brown, J. E. Leavy, J. Jancey, Implementation of GeneXpert for TB testing in low- and middle-income countries: A systematic review. *Glob. Health Sci. Prac.* **9**, 698–710 (2021).
61. T. Nalugwa, P. B. Shete, M. Nantale, K. Farr, C. Ojok, E. Ochom, F. Mugabe, M. Joloba, D. W. Dowdy, D. A. J. Moore, J. L. Davis, A. Cattamanchi, A. Katamba, Challenges with scale-up of GeneXpert MTB/RIF® in Uganda: A health systems perspective. *BMC Health Serv. Res.* **20**, 162 (2020).
62. N. L. Rendell, S. Bekhbat, G. Ganbaatar, M. Dorjravdan, M. Pai, C. C. Dobler, Implementation of the Xpert MTB/RIF assay for tuberculosis in Mongolia: A qualitative exploration of barriers and enablers. *PeerJ* **5**, e3567 (2017).
63. WHO, "WHO Consolidated Guidelines on Tuberculosis - Module 3: Diagnosis - Rapid Diagnostics for Tuberculosis Detection" (2021).
64. J. M. Hong, H. Lee, N. V. Menon, C. T. Lim, L. P. Lee, C. W. M. Ong, Point-of-care diagnostic tests for tuberculosis disease. *Sci. Transl. Med.* **14**, eabj4124 (2022).
65. Africa Medical Supplies Platform, GeneXpert IV-4 desktop (2024).
66. HACH, GeneXpert IV, 2 module configuration with laptop (2024).
67. Stop TB Partnership, *GDF January 2024 Diagnostics, Medical Devices & Other Health Products Catalog* (2024).
68. S. M. Graham, L. E. Cuevas, P. Jean-Philippe, R. Browning, M. Casenghi, A. K. Detjen, D. Gnanashanmugam, A. C. Hesseling, B. Kampmann, A. Mandalakas, B. J. Marais, M. Schito, H. M. L. Spiegel, J. R. Starke, C. Worrell, H. J. Zar, Clinical case definitions for classification of intrathoracic tuberculosis in children: An update. *Clin. Infect. Dis.* **61**, S179–S187 (2015).

Acknowledgments: We would like to thank the Tulane National Primate Research Center for help with BSL-3 experiments. BioRender was used to create schemes. **Funding:** Funding for this study was obtained from the National Cancer Institute, U01CA252965 to T.Y.H.; the Eunice Kennedy Shriver National Institute of Child Health and Human Development, R01HD090927 to T.Y.H. and C.J.L. and R01HD103511 to C.J.L.; the National Institute of Allergy and Infectious Diseases, R01AI144168, R01AI175618, R01AI173021, and R01AI177986 to T.Y.H., R01AI174964 to T.R. and R.S.G., R01AI179714 to S.L., and 1R21AI169582-01A1 to B.N.; the NIH, 5R01AI141500 to T.R.; the US Department of Defense, W8IXWH1910026 to T.Y.H.; the German Center of Infection Research (DZIF), TTU-TB 02.709 to C.L.; and the National Institute of Neurological Disorders and Stroke, R21NS130542 to T.Y.H. **Author contributions:** B.M.Y., J.S., B.N., and T.Y.H. conducted study conceptualization. B.M.Y., J.S., and T.J.C. conducted methodology. B.M.Y., J.S., Y.K., J.F., and T.J.C. conducted investigation. B.M.Y. and B.N. conducted visualization. T.Y.H., B.N., T.R., C.J.L., R.S.G., and S.L. conducted funding acquisition. T.Y.H. and B.N. conducted project administration and supervision. B.M.Y. wrote the original draft; B.M.Y., C.J.L., B.N., T.Y.H., T.R., D.G.C., and R.S.G. reviewed and edited the original draft; and J.O., N.H., R.C., C.V., R.S.G., S.L., J.R., C.L., D.G.C., E.P.-T., E.A.G., C.D.M., T.R., B.N., and T.Y.H. conducted resource acquisition. **Competing interests:** B.M.Y., J.S., B.N., and T.Y.H. have submitted a patent application titled "Method and device for portable detection of active TB" (63/768,870). T.Y.H. is a cofounder of IntelliGenome LLC, which is in negotiations to license this patent. T.R. received salary support and travel cost reimbursement according to the terms of a service contract between FIND (a nonprofit organization) and his home institution, UC San Diego. T.R. is a cofounder, board member, and unpaid shareholder of Verus Diagnostics Inc., a company that was founded with the intent of developing diagnostic assays. Verus Diagnostics was not involved in any way with data collection, analysis, or publication of the results of this manuscript. T.R. has not received any financial support from Verus Diagnostics. The UC San Diego Conflict of Interest office has reviewed and approved T.R.'s role in Verus Diagnostics Inc. All other authors declare that they have no competing interests. **Data and materials availability:** All data associated with this study are present in the paper or the Supplementary Materials. Code used in this study has been uploaded to Zenodo at https://doi.org/10.5281/zenodo.14901582.

Submitted 4 April 2024
Resubmitted 28 December 2024
Accepted 19 March 2025
Published 9 April 2025
10.1126/scitranslmed.adp6411

Downloaded from https://www.science.org at Tulane University on April 09, 2025